Journal for Geometry and Graphics
Volume 29 (2025), No. 1, 79–88

Steffen's Flexible Polyhedron Is Embedded. A Proof via Symbolic Computations

Victor Alexandrov, Evgenii Volokitin

Sobolev Institute of Mathematics, Novosibirsk, Russia
and Novosibirsk State University, Novosibirsk, Russia
alex@math.nsc.ru, volok@math.nsc.ru

Abstract. A polyhedron is flexible if it can be continuously deformed preserving the shape and dimensions of each face. In the late 1970's Klaus Steffen constructed a sphere-homeomorphic embedded flexible polyhedron with triangular faces and with 9 vertices only, which is well-known in the theory of flexible polyhedra. At about the same time, a hypothesis was formulated that the Steffen polyhedron has the least possible number of vertices among all embedded flexible polyhedra without boundary. A counterexample to this hypothesis was constructed by Matteo Gallet, Georg Grasegger, Jan Legerský, and Josef Schicho in 2024 only. Surprisingly, until now, no proof has been published in the mathematical literature that the Steffen polyhedron is embedded. Probably, this fact was considered obvious to everyone who made a cardboard model of this polyhedron. In this article, we prove this fact using computer symbolic calculations.

Key Words: Euclidean space, flexible polyhedron, embedded polyhedron, symbolic computations

MSC 2020: 52C25 (primary), 52B70, 51M20

1 Introduction

Let K be a connected 2-dimensional simplicial complex with or without boundary. Depending on the context, a *polyhedron* is either a continuous map $f\colon K \to \mathbb{R}^3$ which is affine linear and nondegenerate on every simplex or the image $f(K) \subset \mathbb{R}^3$ of K. A polyhedron is *embedded* (or *self-intersection free*) if f is injective. A polyhedron $P_0\colon K \to \mathbb{R}^3$ is *flexible* if there are $\varepsilon > 0$ and a continuous family $\{P_t\}_{t\in(-\varepsilon,\varepsilon)}$ of polyhedra $P_t\colon K \to \mathbb{R}^3$ such that, for every $t \neq 0$, $P_t(\sigma)$ is congruent to $P_0(\sigma)$ for every $\sigma \in K$, while $P_t(K)$ and $P_0(K)$ themselves are not congruent to each other. The family $\{P_t\}_{t\in(-\varepsilon,\varepsilon)}$ is a (nontrivial) *flex* of P_0, and t is a *parameter* of the flex.

The first examples of flexible polyhedra without boundary in $\mathbb{R}^3$ were constructed by Raoul Bricard in 1897 in [4]. Nowadays they are called *Bricard octahedra* since, for all of

ISSN 1433-8157/

them, K is equivalent to the natural simplicial complex of a regular octahedron. Every Bricard octahedron has self-intersections.

The first example of an embedded flexible polyhedron without boundary in $\mathbb{R}^3$ was constructed by Robert Connelly in 1977 in [5]; it has 18 vertices and its simplicial complex K is homeomorphic to the sphere.

In 1978, Klaus Steffen constructed an example of an embedded sphere-homeomorphic flexible polyhedron with only 9 vertices. Though Steffen never published his example in a mathematical journal, nowadays it is widely known as the Steffen polyhedron. For a long period of time the Steffen polyhedron was supposed to have the least possible number of vertices among all embedded flexible polyhedra without boundary. A counterexample was constructed by Matteo Gallet, Georg Grasegger, Jan Legerský, and Josef Schicho in 2024 only, see [9].

Surprisingly, until now, no proof has been published in the mathematical literature that the Steffen polyhedron is embedded. Probably, the reason is that this fact is considered obvious to everyone who made a cardboard model of this polyhedron.

In this article, we give the first proof of this fact. Our proof is based on computer symbolic calculations. The corresponding algorithm was previously presented in our article [2] (for the study of another problem) and in our post [3] (for the study of the embeddedness of the Steffen polyhedron, but many mathematical details were omitted there).

2 The Steffen Polyhedron S_0

In Section 2 we briefly explain what the Steffen polyhedron is. The easiest way to do this is to explain how to build its cardboard model. Another approach to introduce the Steffen polyhedron to the reader is realized in [1].

A cardboard model of the Steffen polyhedron can be glued from the development shown in Fig. 1. The gluing instructions and explanations are given in the caption under the figure.

When gluing, it is useful to keep in mind the following two facts, for which we refer the reader to [1]:

(a) after performing all the gluings $a, \dots, h$, the spatial distance between the vertices v_3 and v_4 is automatically set to 11 (this is not immediately obvious from Fig. 1, because v_3 and v_4 are not connected by an edge);

(b) after performing the gluings $a, \dots, f$, but not the gluings g and h, both the vertex v_9 of the triangle $\{v_5, v_6, v_9\}$ and the vertex v_9 of the triangle $\{v_7, v_8, v_9\}$ can move independently of each other along a circle, γ, which is the intersection of two spheres of the same radius 10; one sphere is centered at v_3, the other at v_4.

We call the *Steffen polyhedron* S_0 a polyhedron glued from the development shown in Fig. 1 in accordance with the gluing instructions given in the caption under Fig. 1 and such that its vertex v_9 is located on the ray coming out of the midpoint of the segment $\{v_3, v_4\}$ and passing through the the midpoint of the segment $\{v_1, v_2\}$.

Let us introduce a right-handed Cartesian coordinate system in Euclidean 3-space such that its origin 0 coincides with the midpoint of $\{v_3, v_4\}$ and its positive x- and z-semiaxis pass through the point v_4 and the middle point of $\{v_1, v_2\}$, respectively; see Fig. 2. In this article, we use coordinates of points relative to this coordinate system only.

By definition, put $v_j = (x_j, y_j, z_j)$ for every $j = 1, \dots, 9$.

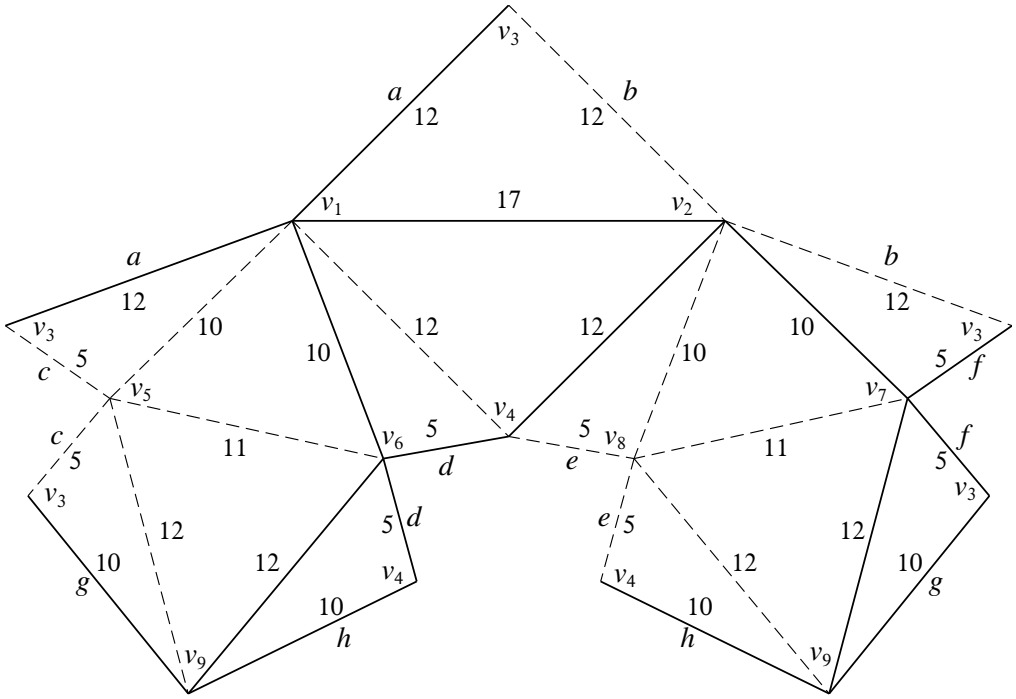

Figure 1: Development of the Steffen polyhedron. Solid lines represent mountain folds, dash lines are valley folds. Integer numbers (other than subscripts) indicate edge lengths. Symbols v_j indicate vertices, $j = 1, \ldots, 9$. Letters $a, \ldots, h$, written outside the development, provide gluing instructions.

The coordinates of the vertices $v_1, \ldots, v_4$, and v_9 are known to us from the above:

$$\begin{aligned} v_1 &= \left(0, -\frac{17}{2}, \frac{\sqrt{166}}{2}\right); \quad v_2 = \left(0, \frac{17}{2}, \frac{\sqrt{166}}{2}\right); \\ -v_3 = v_4 &= \left(\frac{11}{2}, 0, 0\right); \quad v_9 = \left(0, 0, -\frac{3\sqrt{31}}{2}\right). \end{aligned} \tag{1}$$

To find the coordinates of the remaining vertices $v_5, \ldots, v_8$, we note that, for every $j = 5, \ldots, 8$, v_j is connected by an edge to some three vertices among those, whose coordinates are specified in (1). For example, for v_6, these are v_1, v_4, and v_9. Therefore, to find the coordinates of v_6, we solve the following system of algebraic equations

$$\begin{aligned} (x_6 - x_1)^2 + (y_6 - y_1)^2 + (z_6 - z_1)^2 &= 10^2, \\ (x_6 - x_4)^2 + (y_6 - y_4)^2 + (z_6 - z_4)^2 &= 5^2, \\ (x_6 - x_9)^2 + (y_6 - y_9)^2 + (z_6 - z_9)^2 &= 12^2 \end{aligned} \tag{2}$$

with respect to x_6, y_6, and z_6. We solve (2) symbolically using the Wolfram Mathematica software system and obtain two solutions (x_6', y_6', z_6') and (x_6'', y_6'', z_6''), which correspond to points v_6' and v_6'' in Euclidean 3-space, which obviously are symmetric to each other with respect to the plane, passing through the vertices v_1, v_4, and v_9. In Fig. 1, the edge $\{v_1, v_2\}$ is a mountain fold, while $\{v_1, v_4\}$ is a valley fold. Hence, the vertices v_3 and v_6 are located in the different halfspaces determined by the plane passing through the vertices v_1, v_2, and v_4; equivalently, we can say that the vectors v_3 and v_6 are such that the following mixed products

$$((v_2 - v_1) \times (v_4 - v_1)) \cdot (v_3 - v_1) \quad \text{and} \quad ((v_2 - v_1) \times (v_4 - v_1)) \cdot (v_6 - v_1) \tag{3}$$

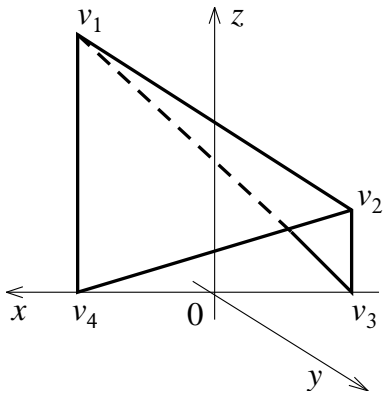

Figure 2: The right-handed Cartesian coordinate system in Euclidean 3-space associated with the Steffen polyhedron S_0.

have opposite signs. So, using (3) and executing symbolic calculations with Wolfram Mathematica, we detect the vertex $v_6 = (x_6, y_6, z_6)$ among the two solutions v_6' and v_6'' to (2). It turns out that

$$\begin{aligned} x_6 &= \frac{258783870279 - 389769468\sqrt{5146} + 102\sqrt{31a}}{51998549858}, \\ y_6 &= \frac{-89746193059 + 533205663\sqrt{5146} - 33\sqrt{31a} - 11\sqrt{166a}}{25999274929}, \\ z_6 &= \frac{6920764197\sqrt{31} + 714577358\sqrt{166} - 187\sqrt{a}}{25999274929}. \end{aligned} \tag{4}$$

where $a = 23829556819105727 + 373057935372156\sqrt{5146}$.

Using similar arguments, we find expressions in radicals for the coordinates of the vertices v_5, v_7, and v_8 through symbolic calculations and use them in Section 4. Those expressions are even longer then the expressions for the coordinates of v_6 in (4) and, thus, are even less informative. So, we omit them, but write the approximate values for the coordinates of $v_5, \ldots, v_8$:

$$\begin{aligned} &v_5 \approx (-1.98248, 0.834943, 3.45397), \quad v_6 \approx (6.89559, -4.79631, 0.218428), \\ &v_7 \approx (-6.89559, 4.79631, 0.218428), \quad v_8 \approx (1.98248, -0.834943, 3.45397). \end{aligned} \tag{5}$$

The main goal of this article is to prove that the Steffen polyhedron S_0 with the vertices $v_1, \ldots, v_9$, the coordinates of which are given in radicals by (1), (4), and by the expressions in radicals, corresponding to (5), is embedded. This goal will be achieved using symbolic calculations described in Sections 3 and 4.

We have already mentioned that the Steffen polyhedron S_0 is flexible. Let us define its flex $\{S_t\}_{t\in(-\varepsilon,\varepsilon)}$ right now. To do this, it suffices to specify the position of each vertex $v_j(t)$ of the polyhedron S_t. By definition, we put $v_j(t) = v_j$ for all $j = 1, \ldots, 4$, and define $v_9(t)$ as the point lying on the circle γ, defined in the property (b) in Section 2, and such that the oriented angle $\angle v_9(t)0v_9$ is equal to t radians; finally, we calculate the coordinates of $v_j(t)$ for all $j = 5, \ldots, 8$, from the coordinates of $v_j(t)$, $j = 1, \ldots, 4$, and $v_9(t)$ in the same way as the coordinates of v_j for $j = 5, \ldots, 8$ were calculated from the coordinates of v_j, $j = 1, \ldots, 4$, and v_9 above. In Section 5 we study some properties of $\{S_t\}_{t\in(-\varepsilon,\varepsilon)}$ using floating point calculations.

3 An Algorithm for Checking Whether a Polyhedron is Embedded

Many algorithms for recognizing self-intersections of polyhedral surfaces are described in the literature; for example, see references in [2]. But their creators optimize performance, memory usage, and other parameters that are not interesting to us; on the other hand they often don't care about the missing a "small", indistinguishable on the screen, self-intersection. This does not suit us in principle, because even the presence of an intersection consisting of a single point changes the answer in our problem to the opposite. Therefore, we had to propose our own algorithm and had to realize it in Wolfram Mathematica, using symbolic computations only. Our algorithm has already been described in [2]. In this section, we describe it in a slightly different way, which is shorter and clearer than the original one.

Lemmas 1 and 2 provide mathematical background for our algorithm.

Lemma 1. *Let K be a connected 2-dimensional simplicial complex with or without boundary, and let $f : K \to \mathbb{R}^3$ be a polyhedron. Then the following statements are equivalent to each other:*

(i) $f(K)$ is not embedded in $\mathbb{R}^3$;

(ii) there are two simplices σ_1, $\sigma_2 \in K$, $\dim \sigma_1 \le 1$, and two points $u_j \in \sigma_j$, $j = 1, 2$, such that $u_1 \ne u_2$, $f(u_1) = f(u_2)$.

Proof. The statement (ii) yields that f is not injective. Hence, $f(K)$ is not embedded, and (i) is true.

Conversely, suppose that (i) holds true. Then f is not injective, i.e., there are two points $\widetilde{u}_j \in K$, $j = 1, 2$, such that $\widetilde{u}_1 \ne \widetilde{u}_2$ and $f(\widetilde{u}_1) = f(\widetilde{u}_2)$. For every $j = 1, 2$, among all simplices in K containing $\widetilde{u}_j$, choose the simplex of the minimum dimension and denote it by $\widetilde{\sigma}_j$. Let us show how to choose σ_1, σ_2, u_1, and u_2, satisfying (ii).

First, consider the case, when $\dim \widetilde{\sigma}_1 < 2$ or $\dim \widetilde{\sigma}_2 < 2$. Swapping, if necessary, the indices $j = 1, 2$ so that $\dim \widetilde{\sigma}_1 \le 1$, we conclude that (ii) is true with $u_j = \widetilde{u}_j$ and $\sigma_j = \widetilde{\sigma}_j$ for $j = 1, 2$.

Now consider the case, when $\dim \widetilde{\sigma}_1 = \dim \widetilde{\sigma}_2 = 2$. For every $j = 1, 2$, $\widetilde{u}_j$ is an interior point of $\widetilde{\sigma}_j$ because $\widetilde{\sigma_j}$ has the minimum dimension among all simplices in K containing $\widetilde{u}_j$. Therefore, the point $f(\widetilde{u}_1) = f(\widetilde{u}_2)$ is an interior point of both the triangle $f(\widetilde{\sigma}_1)$ and the triangle $f(\widetilde{\sigma}_2)$. Hence, $f(\widetilde{\sigma}_1) \cap f(\widetilde{\sigma}_2)$ is not reduced to the single point $f(\widetilde{u}_1) = f(\widetilde{u}_2)$. Let a straight-line segment τ be such that

(A) $\tau \subset f(\widetilde{\sigma}_1) \cap f(\widetilde{\sigma}_2)$;

(B) $f(\widetilde{u}_1) = f(\widetilde{u}_2) \in \tau$; and

(C) τ is maximal with respect to inclusion among all segments satisfying (A) and (B).

Note that at least one endpoint of τ is not contained in the set $f(\widetilde{\sigma}_{12})$, where $\widetilde{\sigma}_{12} = \widetilde{\sigma_1} \cap \widetilde{\sigma_2}$. Indeed, by the definition of simplicial complex, $\widetilde{\sigma}_{12}$ is either an empty set, a 0-dimensional simplex, or a 1-dimensional simplex of K, and, by the definition of polyhedron, $f|_{\widetilde{\sigma}_{12}}$ is a nondegenerate affine linear map. Therefore, assuming that both ends of τ are contained in $f(\widetilde{\sigma}_{12})$, it follows that $\tau \subset f(\widetilde{\sigma}_{12})$. But then the condition $f(\widetilde{u}_1) = f(\widetilde{u}_2) \in \tau$ implies $\widetilde{u}_1 = \widetilde{u}_2$, which contradicts the above assumption $\widetilde{u}_1 \ne \widetilde{u}_2$.

So, at least one endpoint of τ is not contained in $f(\widetilde{\sigma}_{12})$. Let us denote that endpoint by v. Since τ is maximal with respect to inclusion among all segments with the properties (A) and (B), v cannot be an interior point for both the triangle $f(\widetilde{\sigma}_1)$ and the triangle $f(\widetilde{\sigma}_2)$. Swapping, if necessary, the indices $j = 1, 2$, we may assume without loss of generality that v is not an interior point of the triangle $f(\widetilde{\sigma}_1)$. Hence, there is a simplex $\sigma_1 \subset \widetilde{\sigma}_1$,

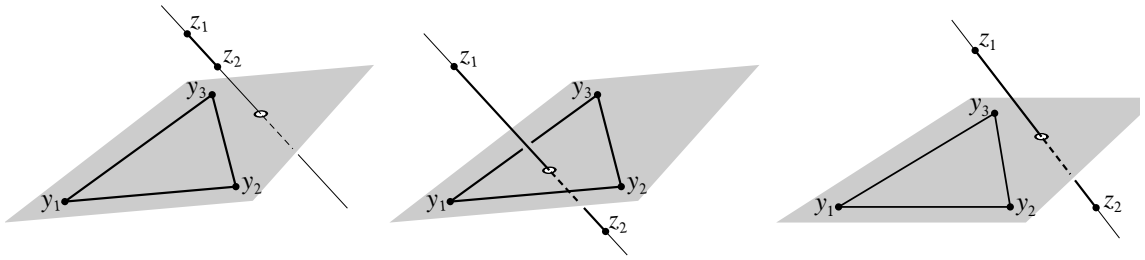

Figure 3: Various cases of mutual arrangement of the triangle $f(\Delta)$ with vertices y_1, y_2, y_3 and the straight-line segment $f(\delta)$ with endpoints z_1, z_2.

$\dim \sigma_1 < \dim \widetilde{\sigma}_1 = 2$, such that $v \in f(\sigma_1)$. Thus, (ii) is true with $u_1 = (f|_{\sigma_1})^{-1}(v) \in \sigma_1$, $u_2 = \widetilde{u}_2 \in \sigma_2$, and $\sigma_2 = \widetilde{\sigma}_2$. □

Informally speaking, Lemma 1 reduces the problem "whether a given polyhedral surface has self-intersections" to the problem "whether a segment and a triangle intersect". Now we begin to study the last one, and we need the following notation.

As is known, if $x_i = (x_{i,1}, x_{i,2}, x_{i,3})$, $i = 0, \dots, 3$, are four points in $\mathbb{R}^3$, then the oriented volume $\mathrm{Vol}(x_0, x_1, x_2, x_3)$ of the tetrahedron $\{x_0, x_1, x_2, x_3\}$ can be calculated using one of the following formulas:

$$\begin{aligned}\mathrm{Vol}(x_0, x_1, x_2, x_3) &= \frac{1}{6}((x_1 - x_0) \times (x_2 - x_0)) \cdot (x_3 - x_0) \\ &= \frac{1}{6}\begin{vmatrix} x_{1,1} - x_{0,1} & x_{1,2} - x_{0,2} & x_{1,3} - x_{0,3} \\ x_{2,1} - x_{0,1} & x_{2,2} - x_{0,2} & x_{2,3} - x_{0,3} \\ x_{3,1} - x_{0,1} & x_{3,2} - x_{0,2} & x_{3,3} - x_{0,3} \end{vmatrix} = \frac{1}{6}\begin{vmatrix} 1 & x_{0,1} & x_{0,2} & x_{0,3} \\ 1 & x_{1,1} & x_{1,2} & x_{1,3} \\ 1 & x_{2,1} & x_{2,2} & x_{2,3} \\ 1 & x_{3,1} & x_{3,2} & x_{3,3} \end{vmatrix}.\end{aligned}$$

In particular, it is a polynomial in variables $x_{i,k}$ ($i = 0, \dots, 3$; $k = 1, 2, 3$). We put by definition $g(x_0, x_1, x_2, x_3) = 6\,\mathrm{Vol}(x_0, x_1, x_2, x_3)$.

Let $f\colon K \to \mathbb{R}^3$ be a polyhedron, and let δ and Δ be 1- and 2-dimensional simplices of K, respectively. We denote the vertices of the closed triangle $f(\Delta)$ by $y_k = (y_{k,1}, y_{k,2}, y_{k,3}) \in \mathbb{R}^3$, $k = 1, \dots, 3$, and denote the endpoints of the closed straight-line segment $f(\delta)$ by $z_j = (z_{j,1}, z_{j,2}, z_{j,3}) \in \mathbb{R}^3$, $j = 1, 2$.

Lemma 2. *With the above notation, the following statements are true*

(α) if $g(y_1, y_2, y_3, z_1)g(y_1, y_2, y_3, z_2) > 0$, then $f(\delta) \cap f(\Delta) = \varnothing$;

(β) if $g(y_1, y_2, y_3, z_1)g(y_1, y_2, y_3, z_2) < 0$, and, in addition, $g(z_1, z_2, y_2, y_3)$, $g(z_1, z_2, y_3, y_1)$, and $g(z_1, z_2, y_1, y_2)$ are nonzero and have one and the same sign, then $f(\delta) \cap f(\Delta) \neq \varnothing$;

(γ) if $g(y_1, y_2, y_3, z_1)g(y_1, y_2, y_3, z_2) < 0$, and, in addition, $g(z_1, z_2, y_2, y_3)$, $g(z_1, z_2, y_3, y_1)$, and $g(z_1, z_2, y_1, y_2)$ are nonzero, but not all of them have one and the same sign, then $f(\delta) \cap f(\Delta) = \varnothing$.

Proof. The statement (α) is true because if $g(y_1, y_2, y_3, z_1)g(y_1, y_2, y_3, z_2) > 0$, then z_1 and z_2 lie on one side of the plane containing the triangle $f(\Delta) = \{y_1, y_2, y_3\}$ (see the left part of Fig. 3).

Now let us assume that the conditions of the statement (β) are fulfilled. Since

$$g(y_1, y_2, y_3, z_1)g(y_1, y_2, y_3, z_2) < 0,$$

the points z_1 and z_2 lie on different sides of the plane containing the triangle $f(\Delta) = \{y_1, y_2, y_3\}$ (see the center and right parts of Fig. 3). For each point x on the boundary of $f(\Delta)$, denote by $\pi(x)$ the halfplane bounded by the line containing $f(\delta)$ and passing through x. Since $g(z_1, z_2, y_2, y_3)$, $g(z_1, z_2, y_3, y_1)$, and $g(z_1, z_2, y_1, y_2)$ have the same sign, then if x goes around the boundary of $f(\Delta)$ once, moving all time in the same direction, then the halfplane $\pi(x)$ also always rotates in the same direction and makes a complete turn around the straight line including $f(\delta)$. This means that the boundary of $f(\Delta)$ is linked to the straight line including $f(\delta)$. Taking into account that the endpoints of $f(\delta)$ lie on the opposite sides of the plane containing $f(\Delta)$, we conclude that $f(\delta) \cap f(\Delta) \neq \varnothing$. Hence, (β) is proved. This case is schematically shown in the center part of Fig. 3.

We treat the case (γ) similarly to (β). But this time the halfplane $\pi(x)$ does not always rotate in the same direction and therefore does not make a complete turn around the straight line including $f(\delta)$. Therefore, $f(\delta) \cap f(\Delta) = \varnothing$, and (γ) is proved. This case is schematically shown in the right part of Fig. 3. □

Lemma 2 solves the problem "whether a given segment and triangle intersect" in many cases, but not in all. We say that the latter are "cases requiring additional study". We hope that in reality there will be few or no such cases. Therefore, we do not want to complicate our algorithm; it suit us if, when such a case occurs, the algorithm informs us about it and continues its work.

Now let us describe our algorithm.

The algorithm accepts four files as input: a list `s` of the 1-dimensional simplices of K; a list `ss` of the edges of $f(K) \subset \mathbb{R}^3$ with the coordinates of their endpoints; a list `t` of the 2-dimensional simplices of K; and a list `tt` of the faces of $f(K) \subset \mathbb{R}^3$ with the coordinates of their vertices.

Our algorithm performs a complete search for all pairs (δ, Δ), where $\delta \in$ `s` and $\Delta \in$ `t`. When (δ, Δ) is fixed, proceed as follows:

⟨1⟩ If $\delta \subset \Delta$, then go to ⟨8⟩; else go to ⟨2⟩. [At this step we conclude that this situation makes no contribution to the set of self-intersections of $f(K)$]

⟨2⟩ Pick up the coordinates of the endpoints z_1 and z_2 of $f(\delta)$ from the list `ss` and the coordinates of the vertices y_1, y_2, and y_3 of $f(\Delta)$ from the list `tt`. If $\delta \cap \Delta$ consists of a single point, u, then go to ⟨3⟩; else go to ⟨4⟩. [At this step we introduce notation and switch between two cases]

⟨3⟩ Change, if necessary, the indices 1, 2, and 3 so that $y_1 = z_1 = f(u)$; if $g(y_1, y_2, y_3, z_2) \neq 0$ then go to ⟨4⟩; else add the line "The case of (δ, Δ) requires additional study" to the output file `out1` and go to ⟨8⟩. [At this step we study the case when $\delta \cap \Delta$ consists of a single point]

⟨4⟩ If $g(y_1, y_2, y_3, z_1)g(y_1, y_2, y_3, z_2) > 0$, then go to ⟨8⟩; else go to ⟨5⟩. [At this step we study the case when $\delta \cap \Delta = \varnothing$; according to the case (α) of Lemma 2, we conclude that that this situation makes no contribution to the set of self-intersections of $f(K)$]

⟨5⟩ If $g(y_1, y_2, y_3, z_1)g(y_1, y_2, y_3, z_2) < 0$ and $g(z_1, z_2, y_2, y_3)$, $g(z_1, z_2, y_3, y_1)$, and $g(z_1, z_2, y_1, y_2)$ are nonzero and have one and the same sign, then add the line "The edge $f(\delta)$ intersects the face $f(\Delta)$" to the output file `out2`, and go to ⟨8⟩; else go to ⟨6⟩. [At this step we use the case (β) of Lemma 2, and conclude that that this situation contributes to the set of self-intersections of $f(K)$]

⟨6⟩ If $g(y_1, y_2, y_3, z_1)g(y_1, y_2, y_3, z_2) < 0$ and $g(z_1, z_2, y_2, y_3)$, $g(z_1, z_2, y_3, y_1)$, and $g(z_1, z_2, y_1, y_2)$ are nonzero, but not all of them have one and the same sign, then go to ⟨8⟩; else go

to ⟨7⟩. [At this step we use the case (γ) of Lemma 2, and conclude that this situation makes no contribution to the set of self-intersections of $f(K)$]

⟨7⟩ Add the line "The case of (δ, Δ) requires additional study" to the output file `out1` and go to ⟨8⟩. [This step corresponds to situations not covered by Lemma 2]

⟨8⟩ If (δ, Δ) is the last item in the complete search, then go to ⟨9⟩; else choose the next pair (δ, Δ) and go to ⟨1⟩.

⟨9⟩ Save the output files, `out1` and `out2`, and quit.

4 Studying the Embeddedness of the Steffen Polyhedron S_0 via Symbolic Calculations

We have implemented the algorithm described in Section 3 as a program in the software system Wolfram Mathematica. The full text of this program is available in [3].

Recall that throughout this article, the Steffen polyhedron S_0 is the polyhedron constructed in Section 2 from the development shown in Fig. 1. In particular, in the coordinate system constructed in Section 2, the vertex v_9 of S_0 is located on the z-axis and has a negative z-coordinate.

The lists `s` and `t` of 1- and 2-dimensional simplices of K, mentioned in Section 3, are compiled directly from the development of S_0, shown in Fig. 1. In Section 3 we explained in detail how we find the coordinates of all the vertices $v_1, \ldots, v_9$ of S_0 in rational numbers or in radicals. Using these coordinates, we prepare the list `ss` of the edges of $f(K) \subset \mathbb{R}^3$ with the coordinates of their endpoints and the list `tt` of the faces of $f(K) \subset \mathbb{R}^3$ with the coordinates of their vertices.

Using the lists `s`, `t`, `ss`, and `tt` as input data for our program and performing all calculations symbolically (i.e. without using floating point arithmetic), we get two empty output files `out1` and `out2`. This means that the program does not find in S_0 intersections and cases requiring additional study. On this basis, we consider the following theorem to be proved:

Theorem 1. *The Steffen polyhedron S_0 is embedded (i.e., S_0 has no self-intersections).* □

Since we know the coordinates of all the vertices of S_0 in rational numbers or in radicals, it is not difficult for us to find its volume in radicals. To do this, we represent the volume of S_0 as the sum of the oriented volumes of 14 tetrahedra, each of which has the origin of the coordinate system as its apex and some face of S_0 as its base. (Of course, the orientation of each tetrahedron must be inherited from a fixed orientation of S_0.) Symbolic computations in Wolfram Mathematica show that the volume of S_0 is equal to $187\sqrt{83}/(6\sqrt{2})$. It is interesting to note that the same number, $187\sqrt{83}/(6\sqrt{2})$, is equal to the volume of the tetrahedron whose vertices are the vertices v_1, v_2, v_3, and v_4 of the Steffen polyhedron S_0, see (1), and Figs. 1 and 2.

5 Numerical Study of the Flex $\{S_t\}_{t\in(-\varepsilon,\varepsilon)}$

Recall that, in the last paragraph of Section 2, we defined a flex $\{S_t\}_{t\in(-\varepsilon,\varepsilon)}$ of the Steffen polyhedron S_0 by specifying the position of each vertex $v_j(t)$ of the polyhedron S_t. Namely, we put $v_j(t) = v_j$ for all $j = 1, \ldots, 4$, and define $v_9(t)$ as the point lying on the circle γ, defined in the property (b) in Section 2, and such that the oriented angle $\angle v_9(t)0v_9$ is equal to t radians. Since lengths of all edges of the Steffen polyhedron are known to us, the above

data is sufficient to compute the coordinates of the points $v_j(t)$ for every $j = 5, \dots, 8$, from the coordinates of the points $v_j(t)$, $j = 1, \dots, 4$, and $v_9(t)$.

In Section 4 we used Lemma 2 in order to conclude that S_0 is embedded, i.e., our arguments were based on some combinations of inequalities involving the values of the polynomial g. By continuity, the same inequalities hold true for the values of g calculated for S_t for every t close enough to zero. Thus, S_t is embedded for all such t. Naturally, we want to have a quantitative estimate for the maximum t for which S_t is embedded.

In Section 5 we present the results of our study of the problem "what is the maximum value of $\varepsilon > 0$ such that S_t has no self-intersections for all $t \in (-\varepsilon, \varepsilon)$?" In other words, in this Section we want to understand how big the angle $\angle v_9(t)0v_9$ can be made so that S_t is still embedded.

Unfortunately, we can only answer this question using floating point calculations.

We put $t = \arcsin(9/40) \approx 0.226943 \approx 13.0029^\circ$ and apply our program in Wolfram Mathematica mentioned in Section 4, which implements our algorithm described in Section 3. Using floating point calculations we see that S_t has no self-intersections.

Similarly, for $t = \arcsin(19/80) \approx 0.239791 \approx 13.739^\circ$ numerical calculations show that S_t has self-intersections. Moreover, our program informs us that self-intersections occur because the edge $\{v_2(t), v_3(t)\}$ intersects the face $\{v_7(t), v_8(t), v_9(t)\}$, and $\{v_7(t), v_8(t)\}$ intersects $\{v_1(t), v_2(t), v_3(t)\}$.

Therefore, we can conjecture that $v_9(t)$ can be moved along the circle γ per angle up to 13° in both directions from the point $v_9 = v_9(0)$ so that S_t is embedded. In other words, the range of the displacements of $v_9(t)$ for which S_t is embedded, is at least $9\sqrt{2621}/100 \approx 4.60761$. Note that this value is comparable to 5, i.e., to the length of the shortest edges of S_t.

6 Concluding Remarks

The theory of flexible polyhedra began with Bricard's article [4]. Its heyday started after Connelly's article [5]. The most famous result of the theory of flexible polyhedra states that the volume of any flexible closed orientable polyhedron in $\mathbb{R}^n$, $n \geq 3$, remains constant during the flex, see, for example, Gaifullin's overview article [6]. This theory is also being developed in non-Euclidean spaces, see, for example, [7].

The theory of flexible polyhedra is attractive because everyone can find here an open problem of any level of difficulty that would suit their mathematical tastes and background. Below we pose two open problems related to the topic of this article.

Recall that two embedded polyhedra in $\mathbb{R}^3$ are called scissors-congruent if the finite part of the space bounded by the first polyhedron can be cut into finitely many tetrahedra that can be reassembled to yield the finite part of the space bounded by the second polyhedron.

The first problem develops the well-known fact that if one embedded polyhedron is obtained from another by a flex, then they are scissors-congruent, see [8]. Hence, the Steffen polyhedron S_0 is scissors-congruent to every polyhedron S_t constructed in the last paragraph of Section 2 with t close enough to zero (so that S_t is embedded).

Open problem 1: For a given t close enough to zero, explicitly specify the partition of S_0 into a finite set of tetrahedra from which S_t can be reassembled.

In Section 4 we observed that the volume of the Steffen polyhedron S_0 is equal to the volume of the tetrahedron, whose vertices are the vertices v_1, v_2, v_3, and v_4 of S_0. This naturally gives rise to the following

Open problem 2: Are the Steffen polyhedron S_0 and the tetrahedron $\{v_1, v_2, v_3, v_4\}$ scissors-congruent? If yes, explicitly specify the partition of $\{v_1, v_2, v_3, v_4\}$ into a finite set of tetrahedra from which S_0 can be reassembled.

In conclusion, the authors declare that all symbolic and numerical calculations performed in the preparation of this article were executed using the computer software system Wolfram Mathematica 12.1 [10], license 3322–8225.

Acknowledgment:

The research was carried out within the State Task to the Sobolev Institute of Mathematics (Project FWNF–2026–0026).

References

[1] V. Alexandrov: *The Dehn invariants of the Bricard octahedra*. Journal of Geometry **99**(1–2), 1–13, 2010. doi: 10.1007/s00022-011-0061-7.

[2] V. A. Alexandrov and E. P. Volokitin: *An embedded flexible polyhedron with nonconstant dihedral angles*. Siberian Mathematical Journal **65**(6), 1259–1280, 2024. doi: 10.1134/S003744662406003X.

[3] V. A. Alexandrov and E. P. Volokitin: *Given a polyhedral surface, is it self-intersection-free?* Wolfram Community, Staff picks, 2025. https://community.wolfram.com/groups/-/m/t/3382354.

[4] R. Bricard: *Mémoire sur la théorie de l'octaèdre articulé*. Journal de Mathématiques Pures et Appliquées. 5. Série **3**, 113–148, 1897.

[5] R. Connelly: *A counterexample to the rigidity conjecture for polyhedra*. Publications Mathématiques. Institut des Hautes Études Scientifiques, Bures-sur-Yvette **47**(1), 333–338, 1977. doi: 10.1007/BF02684342.

[6] A. A. Gaifullin: *Flexible polyhedra and their volumes*. In Mehrmann, V. et al., ed., *European Congress of Mathematics. Proceedings of the 7th ECM, Berlin, Germany, July 18–22, 2016*, 63–83. European Mathematical Society, Zürich, 2018. doi: 10.4171/176-1/2.

[7] A. A. Gaifullin: *Exotic spherical flexible octahedra and counterexamples to the Modified Bellows Conjecture*, 2025. arXiv: 2503.09582.

[8] A. A. Gaifullin and L. S. Ignashchenko: *Dehn invariant and scissors congruence of flexible polyhedra*. Proceedings of the Steklov Institute of Mathematics **302**(1), 130–145, 2018. doi: 10.1134/S0081543818060068.

[9] M. Gallet, G. Grasegger, J. Legerský, and J. Schicho: *Pentagonal bipyramids lead to the smallest flexible embedded polyhedron*, 2024. arXiv: 2410.13811.

[10] S. Wolfram: *The Mathematica book. Version 4*. Cambridge University Press, Cambridge, 4th ed., 1999.

Received August 13, 2025; final form August 27, 2025.